J Electroceram (2006) 17:359–363
DOI 10.1007/s10832-006-7111-9

Dielectric, thermal and sintering behavior of BaO-B_2O_3-SiO_2 glasses with the addition of Al_2O_3

Eun-Sub Lim · Byung-Sook Kim · Joon-Hyung Lee · Jeong-Joo Kim

Received: 27 June 2005 / Revised: 5 January 2006 / Accepted: 12 January 2006

Abstract In the Pb-free low temperature sinterable glass of the (55)BaO-(35)B_2O_3-(10)SiO_2 system, different amounts of Al_2O_3 were added and the crystallization behavior, sintering behavior and physical characteristics of the glass were examined. It was found that Al_2O_3 suppressed crystallization of the glasses because it played the role of a network former. The glass transition temperatures, crystallization temperatures, and optimum sintering temperatures increased as the amount of Al_2O_3 increased. In the case of a specimen with a large amount of Al_2O_3, which was not easily crystallized, an over-firing phenomenon was observed when the sintering temperature was higher than the optimum sintering temperature. While the over-firing phenomenon was not observed due to the crystallization in the sample with a little amount of Al_2O_3. The dielectric constant and thermal expansion coefficient of the glasses were also examined and explained in correlation with the crystallization and densification.

Keywords Sintering · Low temperature sinterable glass · Crystallization · Over-firing · Densification

1 Introduction

Significant developments in various electronic industries such as flat panel displays, low-temperature cofired ceramics, and the packaging industry need a variety of new glasses, which can be easily densified at low temperatures [1–3]. Barrier rib material in plasma display panel (PDP) is made up of glass frit-ceramic composites, and PbO containing glasses such as the PbO-B_2O_3-SiO_2 and PbO-B_2O_3-ZnO systems have been popular as a commercial, low temperature sinterable glass [4–6]. Recent nature protection issues, however, restrict the wide use of the PbO system, so that the development of environmentally-friendly materials, which can replace the PbO, has been affected [7–9]. Bi_2O_3, BaO and ZnO have been employed as candidate materials that can replace PbO, particularly in the PbO-B_2O_3-SiO_2 system [7–9]. In this case, in order to obtain low glass transition temperatures, unlike the PbO glass system, much amount of glass network modifier is necessary, thus resulting in glass crystallization [9, 10]. The crystallized phase obviously affects the property and sintering behavior of the glasses. For controllable crystallization, the addition of intermediate Al_2O_3 could be considered [11]. When the molar ratio between the network modifier and intermediate Al_2O_3 is greater than 1, that is, the excessive network modifier is contained in the glass, Al^{3+} ion coordinates with the 4 ions and acts as a network former, and the valence of Al^{3+} is compensated by the network modifier [12]. Therefore, crystallization could be suppressed in glass containing an excessive network modifier since Al_2O_3 is effective as a network former.

In this study, therefore, the Pb-free (55)BaO-(35)B_2O_3-(10)SiO_2 system, which easily crystallizes during sintering, was selected for the application to PDP barrier rib [13]. Different amount of Al_2O_3 was added and the crystallization temperature, glass transition temperature, dielectric constant and thermal expansion coefficient of the glasses were analyzed. The sintering behavior of the glasses was also examined in correlation with crystallization behavior.

2 Experimental

High purity chemicals $BaCO_3$ (99.6%), H_3BO_3 (99.9%), SiO_2 (99.9%) and Al_2O_3 (Kojundo chemical lab co.,

E.-S. Lim · B.-S. Kim · J.-H. Lee · J.-J. Kim (✉)
Department of Inorganic Materials Engineering, Kyungpook National University, Daegu 702-701, Korea
e-mail: jjkim@knu.ac.kr

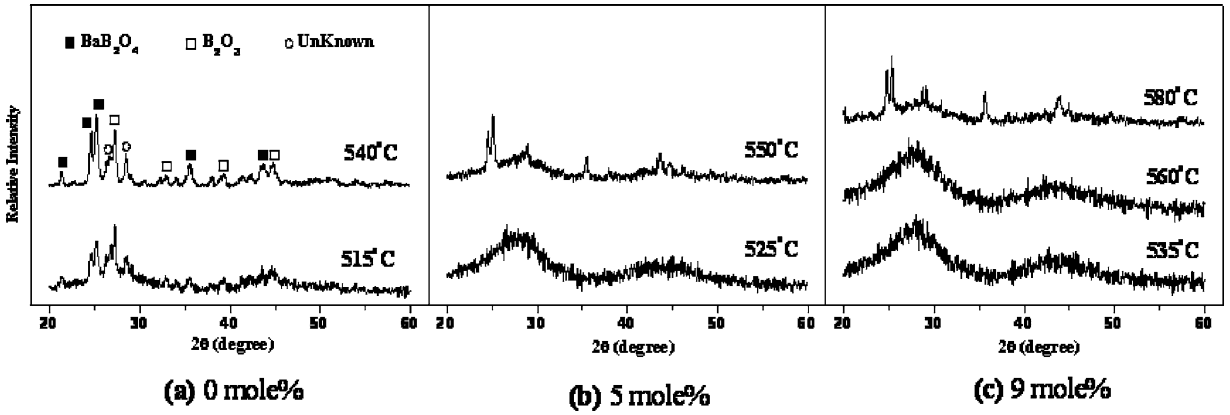

Fig. 1 X-ray diffraction patterns of sintered specimens with (a) 0 mol%, (b) 5 mol% and (c) 9 mol% of Al_2O_3

Ltd, 99.9%, Japan) were used as starting raw materials. The amount of Al_2O_3 in the compositional equation of $(1-x)(55BaO\text{-}35B_2O_3\text{-}10SiO_2)\text{-}(x)Al_2O_3$ was changed where $x = 0, 3, 5, 7, 9$ mol%. Weighed raw powder batches were mixed in an alumina crucible for 15 min and melted at 1200°C for 30 min in a Pt crucible. The molten glass in the crucible was put into cold water for quenching. The glass frit was roughly crushed in an alumina mortar then Planetary-milled for 2 h at 400 rpm. The transition temperature of the glasses was measured by using a DSC (Thermal Analyzer, DSC 2920, TA Instruments, U.S.A).

The glass powders were cold isostatically pressed under a pressure of 100 MPa for 3 min in order to form green pellets. The pellets were sintered at 500–560°C for 2 h with a heating rate of 5°C/min, then they were furnace cooled. The density of the sintered pellets was measured by the Archimedes method. The crystal structure of the glass powders and sintered specimens was analyzed by using an X-ray diffractometer (MO3-XHF, MAC Science Co., Japan). The thermal expansion coefficient of the sintered specimens was measured by using a dilatometer (DIL 402 C, Netzsch, Germany). Dielectric characteristics of the sintered specimens were analyzed by using an impedance gain phase analyzer (HP-4194A, USA) at 1 MHz.

3 Results and discussion

X-ray diffraction patterns of sintered bodies are shown in Fig. 1, for different Al_2O_3 content as a function of sintering temperature. The crystallization of the glass started at 515°C for 0 mol% Al_2O_3, 550°C for 5 mol% Al_2O_3, and 580°C for 9% Al_2O_3. As the amount of Al_2O_3 increased, the crystallization temperature increased. This suggests that Al_2O_3 in the glass acts as a network former and increased the crystallization temperature. In every specimen, the BaB_2O_4 and B_2O_3 phases were crystallized.

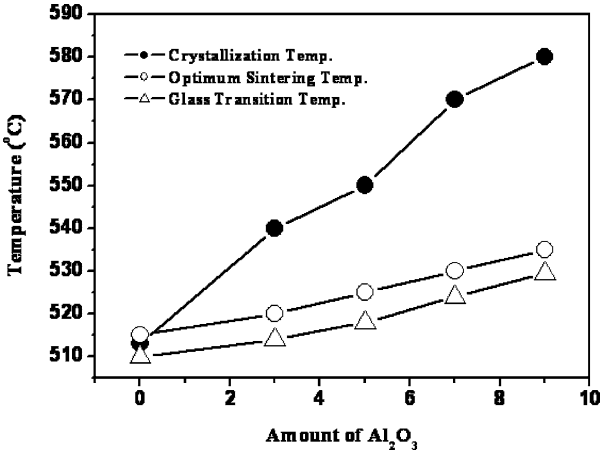

Fig. 2 The effect of the addition of Al_2O_3 on crystallization temperature, optimum sintering temperature and glass transition temperature (°C)

Figure 2 shows the crystallization temperature, optimum sintering temperature, and glass transition temperature, as a function of the Al_2O_3 amounts. These temperatures gradually increased as the amount of Al_2O_3 increased. Note that the crystallization temperature increased more rapidly than the others. The densification behaviors of glasses with different amounts of Al_2O_3 are shown in Fig. 3. The optimum sintering temperature, at which the relative density became its highest value, was observed at a temperature 10°C higher than the glass transition temperature, regardless of the Al_2O_3 content. In the case of the sample without Al_2O_3, crystallization occurred near the optimum sintering temperature of 515°C. However, it was observed that, with the addition of 9 mol% Al_2O_3, crystallization started at 580°C. This was almost 45°C higher than its optimum sintering temperature of 535°C.

Changes in the relative density of the sintered samples are shown in Fig. 3 for different Al_2O_3 content as a function of the sintering temperature. Without Al_2O_3, the sample

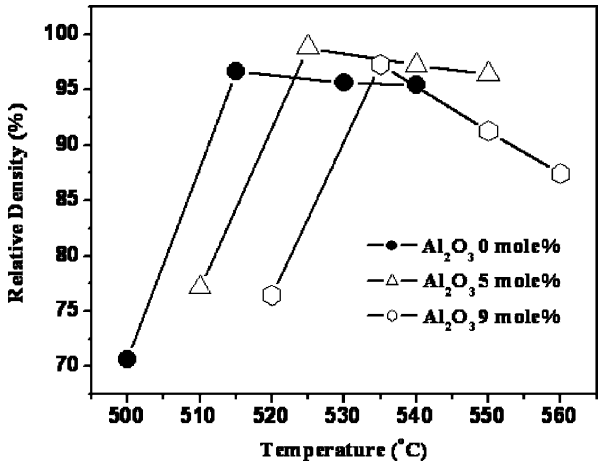

Fig. 3 Relative density (g/cm^3) of specimen sintered at various temperatures

shows its maximum densification at 515°C and the density became almost plateau above the temperature. With the addition of 9 mol% Al_2O_3, however, the relative density rapidly decreases with the sintering temperature above the optimum sintering temperature of 535°C. This is the so-called over-firing phenomenon [14]. It can also be observed that the over-firing phenomenon is facilitated by increasing the amount of Al_2O_3.

Figure 4 shows the SEM images of specimens with 0 mol%, 5 mol%, and 9 mol% Al_2O_3 sintered at their optimum sintering temperatures. Figure 4(a), (b), and (c) were sintered at their optimum sintering temperatures and (d), (e), and (f) were sintered at temperatures 25°C higher than the optimum sintering temperature. Without the addition of Al_2O_3, as shown in Fig. 4(a), the specimen showed the presence of a crystallized phase on the surface which was formed during sintering at its optimum sintering temperature of 515°C. This resulted in high densification with a small amount of pores. Similar densification and crystalline phases were observed at 540°C in Fig. 4(d). For the specimen with the addition of 9 mol% Al_2O_3, crystallization did not occur and the smooth fracture surface, which is the typical feature of glass, was observed after sintering at its optimum sintering temperatures of 535°C and 560°C as shown in Fig. 4(c) and (f). By increasing the temperature above its optimum sintering temperature, however, this gives rise to the formation of large pores as shown in Fig. 4(f). This caused the decrease in the relative density due to the over-firing phenomenon, as shown in Fig. 3. With the addition of 5 mol% Al_2O_3, the specimen, sintered at its optimum sintering temperature of 525°C formed a smooth surface as shown in Fig. 4(b). In Fig. 4(e), however, a rough surface was observed due to the crystallization of the specimen sintered at 550°C. It is also noted that large pores did not form at that temperature. Therefore, the increase in Al_2O_3 suppresses crystallization near the optimum sintering temperature and leads to the over-firing phenomenon of specimens above the optimum sintering temperature.

A schematic diagram, explaining the relationship between over-firing and the crystalline phase, is shown in Fig. 5. When crystallization does not occur at the optimum sintering temperature, increasing the temperature above it causes the coalescence and expansion of pores that lead to the formation of large pores as illustrated in Fig. 5(a). It is generally observed that small isolated pores are generated during the sintering process of glass powders. The small pores can easily move to coalesce with adjacent pores and grow to large pores as the temperature increases because the viscosity of the glass decreases with the temperature. When pore coalescence occurs, it results in an increase in the pore radius and a decrease in pore pressure. Therefore, the volume of the pore after coalescence is larger than the sum of the pore volumes before the coalescence which led to the generation of macro pores [15]. Figure 5(c) shows a case where large pores did not form in the specimen which was crystallized near the optimum sintering temperature even after sintering above the optimum sintering temperature. Generally, the viscosity

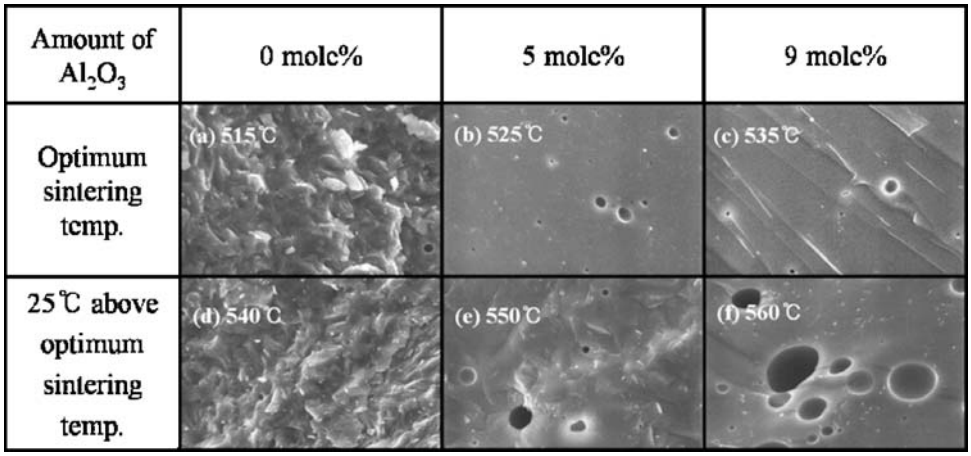

Fig. 4 Fracture surface photographs of samples with (a, d) 0 mol%, (b, e) 5 mol%, and (c, f) 9 mole% of Al_2O_3 sintered at optimum sintering temperature and 25°C above it

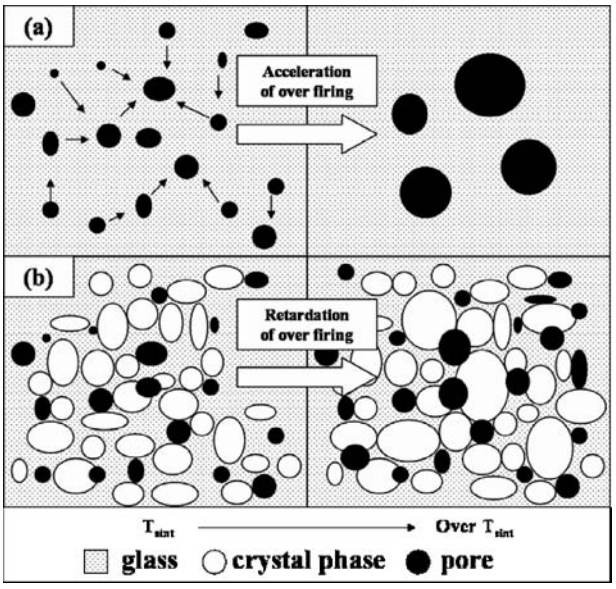

Fig. 5 Schematic diagrams explaining pore coalescence in specimens with and without crystallized phases

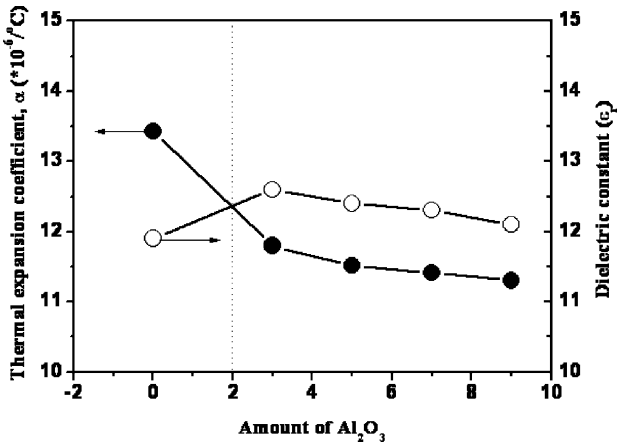

Fig. 6 The effect of the addition of Al_2O_3 on the thermal expansion coefficient (α) and dielectric constant (ε_r)

of the glass increases with the addition of the crystalline solid phase [16]. In the specimens which were crystallized near the optimum sintering temperature, as in the case of the 0 mol% and 5 mol% Al_2O_3 added specimens, the crystalline phase gives rise to a increase of viscosity that hinders the coalescence of the pores. As a result, the suppression of the over-firing phenomenon could be explained by this mechanism.

Figure 6 shows the thermal expansion coefficient (α) and dielectric constant (ε_r) of specimens sintered at their optimum sintering temperatures. In the case of the compositions on the right hand side of the dotted line in Fig. 6, the α decreased gradually from $13.4 \times 10^{-6}/^{\circ}C$ to $11.3 \times 10^{-6}/^{\circ}C$ as the Al_2O_3 content increased. The ε_r also decreased from 12.6 to 12.1. It is thought that the decrease of α is caused by the increase in the content of Al_2O_3, which played the role of a network former. In the case of ε_r, since Al_2O_3 reduced the fraction of nonbridging oxygens, which have high polarity, the ε_r is thought to decrease. On the other hand, in the case of 0 mol% Al_2O_3 on the left hand side of the dotted line, the α was $13.42 \times 10^{-6}/^{\circ}C$, which is higher than the compositions on the right hand side. This seems to be attributed to the crystallization of the BaB_2O_4 phase in the specimen. Since the BaB_2O_4 structure has a high anisotropic α of $36 \times 10^{-6}/^{\circ}C$ along the c axis, the crystallization of the BaB_2O_4 phase obviously affects the α of the specimen. The low ε_r in 0 mol% Al_2O_3 is also believed to be due to the crystallization of the BaB_2O_4 phase since the ε_r of BaB_2O_4 is around 5–8 which is lower than the matrix.

4 Conclusions

In conclusion, the effects of Al_2O_3 on the sintering behavior and properties of the BaO-B_2O_3-SiO_2 glass system are reported. As the amount of Al_2O_3 increased, the crystallization temperature, optimum sintering temperature, and glass transition temperature increased. The addition of Al_2O_3 reduced the amount of the crystalline phase so that the over-firing phenomenon occurred above the optimum sintering temperature. This suggests that the crystalline phase acts as an important role in the densification of glass. The thermal expansion coefficient decreased with the addition of Al_2O_3 because it played the role of a network former and tightened the network structure. The dielectric constant also decreased with the addition of Al_2O_3 due to the reduced the fraction of nonbridging oxygens.

Acknowledgment This work was supported by the National Research Laboratory grant from the Ministry of Science and Technology (MOST) and Korea Science and Engineering Foundation (KOSEF).

References

1. G.H. Hwang, W.Y. Kim, H.J. Jeon, and Y.S. Kim, *Journal of the American Ceramic Society*, **85**, 2961 (2002).
2. H.J. Kim, Y.S. Chung, and K.H. Auh, *Journal of the Korean Association of Crystal Growth*, **9**, 50 (1999).
3. M.J. Pascual, A. Duran, and L. Pascual, *Journal of Non-Crystalline Solids,* **306**, 58 (2002).
4. A. Masashi and K. Shinji, US Patent, 5977708 (1999).
5. H. Naoya and N. Kazuhiro, JP Patent, 11246233 (1999).
6. T.Y. Kim and J.H. Sunwoo, US Patent, 6097151 (2000).
7. Y.H. Jin, Y.W. Jeon, B.C. Lee, and B.K. Ryu, *Journal of the Korean Ceramic Society*, **39**, 184 (2002).
8. C.S. Lee, J.R. Yoo, K.W. Jung, and S.C. Choi, *Journal of the Korean Ceramic Society*, **38**, 628 (2001).
9. D.N. Kim, J.Y. Lee, J.S. Huh, and H.S. Kim, *Journal of Non-Crystalline Solids*, **306**, 70 (2002).

10. B.S. Kim, Y.N. Kim, E.S. Lim, J.H. Lee, and J.J. Kim, *Journal of the Korean Ceramic Society*, **42**, 110 (2005).
11. J.H. Park, S.J. Lee, and J.S. Sung, *Journal of the Korean Ceramic Society*, **29**, 956 (1992).
12. Scholze; Translated by Michael J. Lakin., *Glass: Nature, Structure, and Properties* (Springer-Verlag, New York, 1991), p. 137.
13. E.S. Lim, B.S. Kim, J.H. Lee, and J.J. Kim, *The 4th International Meeting on Information Display*, 1099 (2004).
14. D.H. Park, B.C. Kim, J.J. Kim, and L.S. Park, *Journal of the Korean Ceramic Society*, **37**, 545, (2000).
15. W.D. Kingery, H.K. Bowen, and D.R. Uhlmann, *Introduction to Ceramics*, 2nd edition (Wiley, New York, 1960), p. 206.
16. R.J. Stokes and D.F. Evans, *Fundamentals of Interfacial Engineering* (Wiley, New York, 1997), p. 91.